Chloride Ion as Redox Mediator in Reducing Charge Overpotential of Aprotic Lithium-Oxygen Batteries

Qi Zhang,[a, b] Yin Zhou,[a, b] Wenrui Dai,[a] Xinhang Cui,[b, c] Zhiyang Lyu,[a, d] Zheng Hu,[e] and Wei Chen*[a, b, c, f]

The aprotic lithium-oxygen (Li–O$_2$) battery with a high theoretical energy density has been considered as a promising candidate for next-generation energy storage devices. However, the formation of insulating Li$_2$O$_2$ products is a major obstacle for realizing the high energy efficiency and long cycle life. Here, we report a new Cl$^-$/Cl$_3^-$ redox mediator to reduce the charge overpotential by a facile introduction of chloride ion (Cl$^-$) additives into the organic electrolyte. The redox mediator can effectively promote the formation of the LiOH discharge product, and facilitate efficient LiOH decomposition. Therefore, the cell with the Cl$^-$ additives possesses a significantly low charge overpotential of 0.29 V, an extended cycle life (up to 71 cycles) at a rate of 500 mA g^{-1} with a fixed capacity of 500 mAh g^{-1}, and an enhanced rate capability. This study offers an effective approach to modulate discharge products from Li$_2$O$_2$ to LiOH and provides new insights toward the role of redox mediators through the addition of Cl$^-$ in Li–O$_2$ battery systems.

1. Introduction

Rechargeable aprotic lithium-oxygen (Li–O$_2$) batteries have attracted considerable interest to meet the stringent demand from electric vehicles due to their high theoretical gravimetric energy (~3600 Wh kg^{-1}).[1–2] However, there are many challenges towards the practical development of Li–O$_2$ batteries, such as high charge overpotential, low rate capability, and poor cycling life.[3–6] The key challenge concerning the high charge overpotential is mainly caused by the dominant discharge product of Li$_2$O$_2$, which is intrinsically a wide bandgap insulator with band gap of ~4–5 eV.[7] This can result in the sluggish kinetics of both the charge (oxygen evolution reaction, OER) and discharge (oxygen reduction reaction, ORR) processes.[8] One effective strategy to mitigate this issue is to modulate the Li$_2$O$_2$ discharge products to other products with higher ionic and electronic conductivities, such as LiOH,[9–11] defective-Li$_2$O$_2$,[12–16] LiOOH·H$_2$O,[17–18] and lithium thiosulfate,[19] etc. Among these products, the formation of LiOH can help reduce charge overpotential by enhancing the kinetics of electrochemical oxidation of the newly established battery chemistries. For instance, many groups reported the use of H$_2$O additives to drive the formation of LiOH.[9,20–21] However, the addition of H$_2$O can severely corrode Li anode and degrade the reversibility of aprotic Li–O$_2$ cells.[9,22]

Another effective strategy to reduce the charge overpotential is the addition of the redox mediators (RMs) in the electrolyte to effectively oxidize Li$_2$O$_2$.[23–25] Among the RMs, halides such as lithium iodide (LiI)[26–27] and lithium bromide (LiBr)[28–29] have received wide attention owing to their promising electrochemical reactivity, which involves two redox couples: X$^-$/X$_3^-$ and X$_3^-$/X$_2$. LiI is a well-studied and ideal inorganic redox mediator due to its appropriate redox potential, good chemical stability in conventional organic electrolytes and excellent catalytic capability to decompose Li$_2$O$_2$, thereby achieving a low charge overpotential and high cycling performance.[27,30–32] In addition, some groups suggested that LiI can also promote the formation of LiOH as an energy carrier while its decomposition is aided by LiI$_3$, achieving a low charge potential at around 3.1 V.[11,33–34] Matsuda and coworkers reported that the discharge capacity of a Li–O$_2$ cell with the addition of lithium chloride (LiCl) in the electrolyte was enhanced by nearly 2.5 times.[35] Recently, Deng et al. found that the addition of CuCl$_2$ can act as a multi-functional mobile mediator to enhance the discharge capacity and reduce the

[a] Q. Zhang, Y. Zhou, W. Dai, Dr. Z. Lyu, Prof. W. Chen
Department of Chemistry,
National University of Singapore
3 Science Drive 3, 117543, Singapore
E-mail: phycw@nus.edu.sg

[b] Q. Zhang, Y. Zhou, X. Cui, Prof. W. Chen
National University of Singapore (Suzhou)
Research Institute, 377 Lin Quan Street
Suzhou Industrial Park, Jiang Su, 215123, P. R. China

[c] X. Cui, Prof. W. Chen
Department of Physics,
National University of Singapore
Singapore, 2 Science Drive 3, 117542 Singapore

[d] Dr. Z. Lyu
Jiangsu Key Laboratory for Design and Manufacture
of Micro-Nano Biomedical Instruments
School of Mechanical Engineering,
Southeast University
Nanjing, 211189, China

[e] Prof. Z. Hu
Key Laboratory of Mesoscopic Chemistry of MOE and
Jiangsu Provincial Lab for Nanotechnology
School of Chemistry and Chemical Engineering,
Nanjing University
Nanjing, 210023, P. R. China

[f] Prof. W. Chen
Joint School of National University of Singapore and Tianjin University
International Campus of Tianjin University
Binhai New City, Fuzhou, 350207, P. R. China

charge overpotential by Cu^+/Cu^0 and Cu^+/Cu^{2+} redox couples, respectively.[36] Similarly, Zhang's group combined the tetrathiafulvalene (TTF) and LiCl in the electrolyte to significantly reduce the charge overpotential by generating an organic conductor $TTF^+Cl_x^-$ as an additional electron-transfer pathway.[37] On the basis of the above observations, the addition of Cl^- has shown the improvement of electrochemical behaviors in the Li–O_2 batteries. Therefore, further investigation is required to clarify the effect of chloride additives in this complex Li–O_2 system.

In this work, we systemically investigated the effects of Cl^- additives on the discharge-recharge behaviors of aprotic Li–O_2 batteries by adding LiCl additives into the electrolyte (Figure 1). It is found that the formation of the discharge product LiOH can be promoted from Li_2O_2 by adding the Cl^- additives. Moreover, LiCl can act as a redox mediator to enhance the decomposition of the LiOH discharge product by specific chloride redox species as revealed by X-ray diffraction (XRD), Raman spectroscopy, and scanning electron microscope (SEM) measurements. As a result, the cell with the LiCl additive possesses a significantly low charge overpotential of 0.29 V, an extended cycle life (up to 71 cycles) at a current density of 500 mA g^{-1} with a fixed capacity of 500 mAh g^{-1}, and an enhanced rate capability. This work provides a simple yet effective strategy to enhance battery performance with the added LiCl additives for Li–O_2 batteries.

2. Results and Discussion

2.1. Electrochemical Performance with Chloride Additives

We selected hierarchical carbon nanocages as the cathode materials due to the hierarchical porous architecture, which provides excellent electrical conductivity, large specific surface area,[38–40] and facilities the uniform deposition of discharge products. Figure S1 shows the structural and morphological characterizations for the carbon nanocages. The electrolyte contained 0.45 M $LiClO_4$ and 0.05 M LiCl additives in the

dimethyl sulfoxide (DMSO) solvent. DMSO was selected as it can promote soluble O_2^- formation owing to its high donor number.[41]

Figure 2a shows a comparison of discharge-charge curves for batteries with and without the Cl^- additive. Upon recharging, the cell with Cl^- additive (denoted as CNCs-LiCl) showed a low voltage plateau at ~3.26 V and a low charge overpotential of ~0.3 V when 50% discharge products being decomposed and displayed a high round-trip energy efficiency of ~84.7%. In contrast, the cell under the bare electrolyte (denoted as CNCs) had a high charge overpotential of 1.08 V and a much lower round-trip energy efficiency of ~71.1% (Figure S2). This suggests that the LiCl additive plays a vital role in reducing charge overpotential in Li–O_2 batteries. Moreover, the full discharge/charge capacity was also evaluated. As shown in Figure 2b, the CNCs-LiCl cell delivered a significantly improved discharge capacity of 8386 mAh g^{-1} in comparison with that of the CNCs cell (4522 mAh g^{-1}) and achieved a much lower charge overpotential (~0.3 V). As revealed by the calculated specific energy density in Figure S3, the extended discharge capacity can be rationally ascribed to the discharge product formation. The low charge overpotential is caused by the electrochemical oxidation of discharge products rather than additive Cl^- itself.

The cycling life of Li–O_2 cells with and without Cl^- was investigated with a repeated discharge-charge test at a limited capacity of 500 mAh g^{-1} (Figure 2c, d). Assembled with the bare electrolyte, the cell exhibits large round-trip potential gaps and can only be operated for 23 cycles (Figure 2c). Once the Cl^- additive is introduced, the overpotential is apparently reduced, and the cycling stability is largely improved with 71 stable cycles (Figure 2d). The improved cycling stability of the Li–O_2 cell can be ascribed to the lowered charge overpotential.[28,42–43] Furthermore, the rate capability tests of the Li–O_2 cell in an electrolyte with or without Cl^- were also carried out (Figure 2e, f). As depicted in Figure 2f, the charge voltage of the battery with Cl^- is still maintained below 3.6 V even at a high current density of 1.0 A g^{-1} and the discharge voltage displays minimal
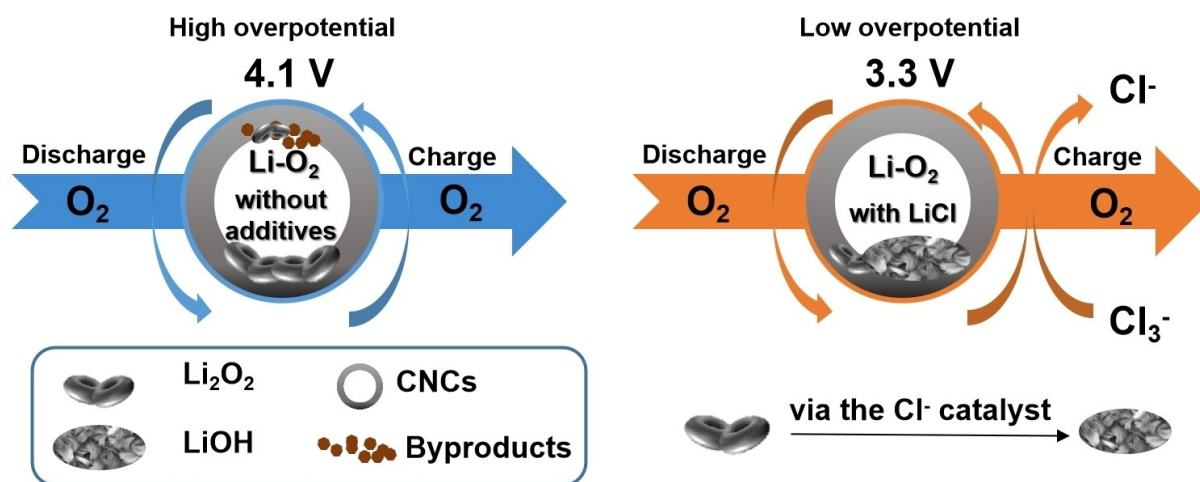

Figure 1. A schematic for Li–O_2 batteries with and without LiCl in the solvent-based on a carbon nanocages cathode. The charge voltage is reduced from 4.1 V to 3.3 V with the addition of the Cl^- ions.
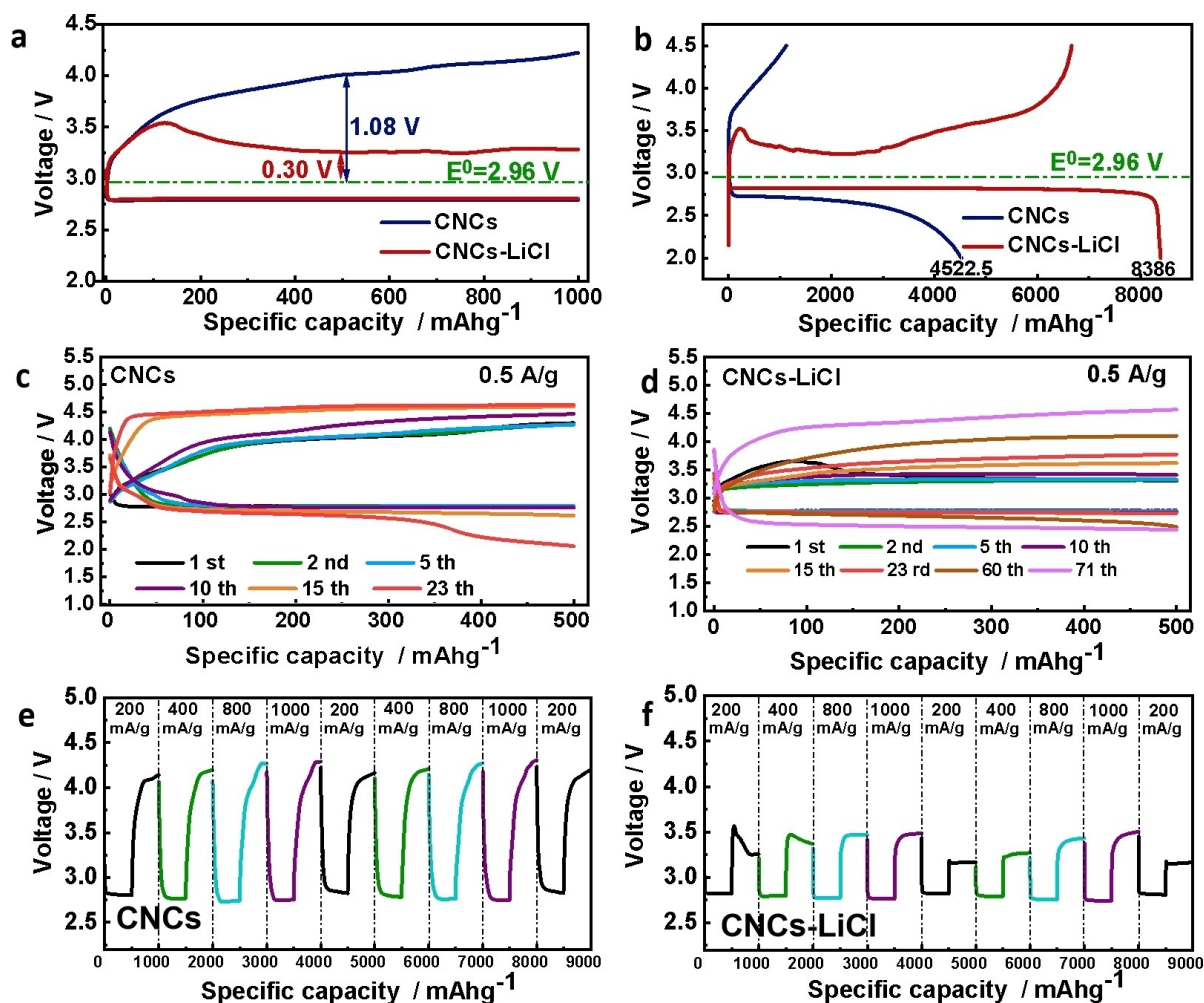
Figure 2. a) The discharge-charge curves of CNCs and CNCs-LiCl cells with a fixed capacity of 1000 mAh g^{-1} (calculated based on the weight of CNCs) at a current density of 100 mA g^{-1}. b) The initial deep discharge-charge curves of CNCs and CNCs-LiCl cells at a current density of 100 mA g^{-1}. Discharge-charge profiles of c) CNCs and d) CNCs-LiCl cathodes with different cycles at 500 mA g^{-1}. The discharge-charge profiles of e) CNCs and f) CNCs-LiCl cells at various current densities ranging from 0.2 to 1.0 A g^{-1} with a limited capacity of 500 mAh g^{-1}.

fluctuations between 2.79 V to 2.75 V with the increasing current rate, revealing a promising high-rate performance. In addition, the electrochemical performance of Cl$^-$ additives in the tetraethylene glycol dimethyl ether (TEGDME) electrolyte is shown in Figure S4. The cycle performance of the CNCs-LiCl cell has been significantly improved to 242 cycles from 37 cycles, with lower charge overpotential. This indicates that the Cl$^-$ can work effectively in other electrolyte systems. It is worth noting that there is an interesting phenomenon for the battery with LiCl additives in DMSO-based electrolytes during the charging process, where a potential barrier appears at the beginning of the first charge, and it disappears in the following cycles (Figure 2d). However, we did not observe a similar phenomenon in TEGDME-based electrolytes with LiCl additives. Thus, we suggest that such an appearance is closely correlated with an activation process that occurred in the fresh LiCl/DMSO electrolyte. More detailed analysis and discussion of the battery performance are presented in the Supporting Information (Figure S4).

2.2. Characterization of the Discharged/Charged Cathodes

The discharge/charge products were fully characterized to further study the battery reversibility (Figure 3). Based on the XRD results for the CNCs cathodes with LiCl in DMSO-based electrolyte (Figure 3a), two diffraction peaks located at around 32.5° and 35.7° appeared after discharging. These peaks exactly correspond to LiOH, which is the only observed crystalline discharge product and can be reversibly decomposed upon recharging. However, the predominant discharge product for CNCs cell is Li$_2$O$_2$ (Figure S5a). This reveals that the discharge mechanism radically changes via the action of Cl$^-$. As shown in Figure 3b, after full discharging, the characteristic Raman peaks at 331, 516, 620, and 1086 cm^{-1} are assigned to the deposited LiOH[44–45] and the Li$_2$O$_2$ Raman signal appears at 790 cm^{-1}.[45] After full charging, all Raman signals related to Li$_2$O$_2$ and LiOH disappear, indicating a reversible electrochemical process. To further verify the reversibility of Li–O$_2$ batteries with CNCs cathodes, SEM measurement was carried out to characterize the products at a different limited depth of discharge/charge
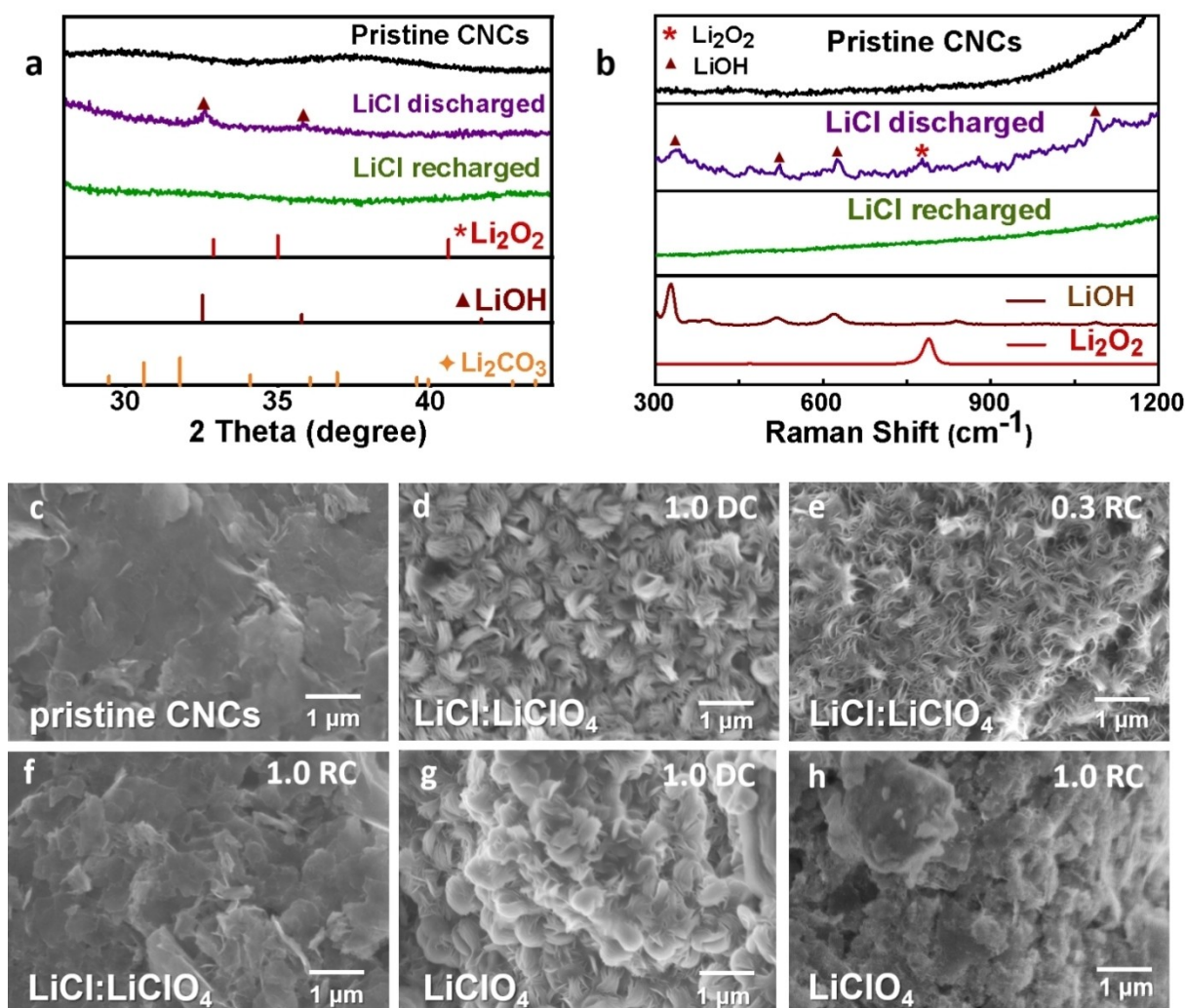
Figure 3. a) XRD pattern of pristine CNCs, full discharged, and recharged cathodes with LiCl additives, and the standard diffraction patterns of various possible products Li_2O_2, LiOH, and Li_2CO_3. b) Raman spectra of different cathodes and commercial LiOH and Li_2O_2 for reference. SEM images of c) as prepared CNCs cathode, d) CNCs-LiCl cathode after discharge, e-f) cathodes after different depth of recharge (RC) denoted by Q/Q_{total} at a fixed Q_{total} of 2.0 mAh with panel (e) for 0.3 recharge and panel (f) for 1.0 recharge, and CNCs cathode without LiCl additives after being g) discharged and h) recharged at a fixed Q_{total} of 2.0 mAh.

(Figure 3c–h). The pristine cathode showed typical morphological characteristics of CNCs (Figure 3c). After discharged to 2.0 mAh, the CNCs cathode without Cl⁻ was covered with numerous toroids with diameters of 500–700 nm (Figure 3g). These typical toroidal discharge products have been confirmed as Li_2O_2 by XRD and Raman (Figure S5). This is also consistent with previous reports, where fast kinetics favors toroid Li_2O_2 formation in the DMSO electrolyte.[46–47] However, in the presence of Cl⁻, the morphology of the discharge products changed to the flower-like structure with obvious layered features. The flower-type shape is regarded as the morphology of LiOH related materials, which is consistent with the previous report.[21] Figure 3e–f show that with increasing depth of recharge for the CNCs-LiCl cathode, the extent of decomposition in the discharge products can be increased gradually, until full decomposition is achieved. However, the cathode of the batteries without Cl⁻ is still covered by the discharge products even as the depth of recharge reaches 1.0 (Figure 3h), in

agreement with the XRD and Raman results in Figure 3a, b. This suggests that the reversibility of the batteries with Cl⁻ can be obviously improved.

2.3. Electrochemical Catalytic Reactivity of Oxidized Chloride Species for Li_2O_2 and LiOH

X-ray photoelectron spectroscopy (XPS) was further used to reveal the chemical composition of the discharge products in the batteries cycled with LiCl. As shown in Figure 4a–b, the peaks at 54.5 eV in Li 1s spectra and 531.2 eV in O 1s spectra can be attributed to Li_2O_2/LiOH, which are consistent with previous reports.[48] More quantitative information on discharge products of both Li_2O_2 and LiOH was obtained by iodometric and acid/base titrations (Figure 4c,d, and Figure S6). The discharge product Li_2O_2 reacts with H_2O through $Li_2O_{2(s)} + 2H_2O_{(l)} \rightarrow H_2O_{2(l)} + 2LiOH_{(aq)}$, where H_2O_2 further oxidizes iodide to
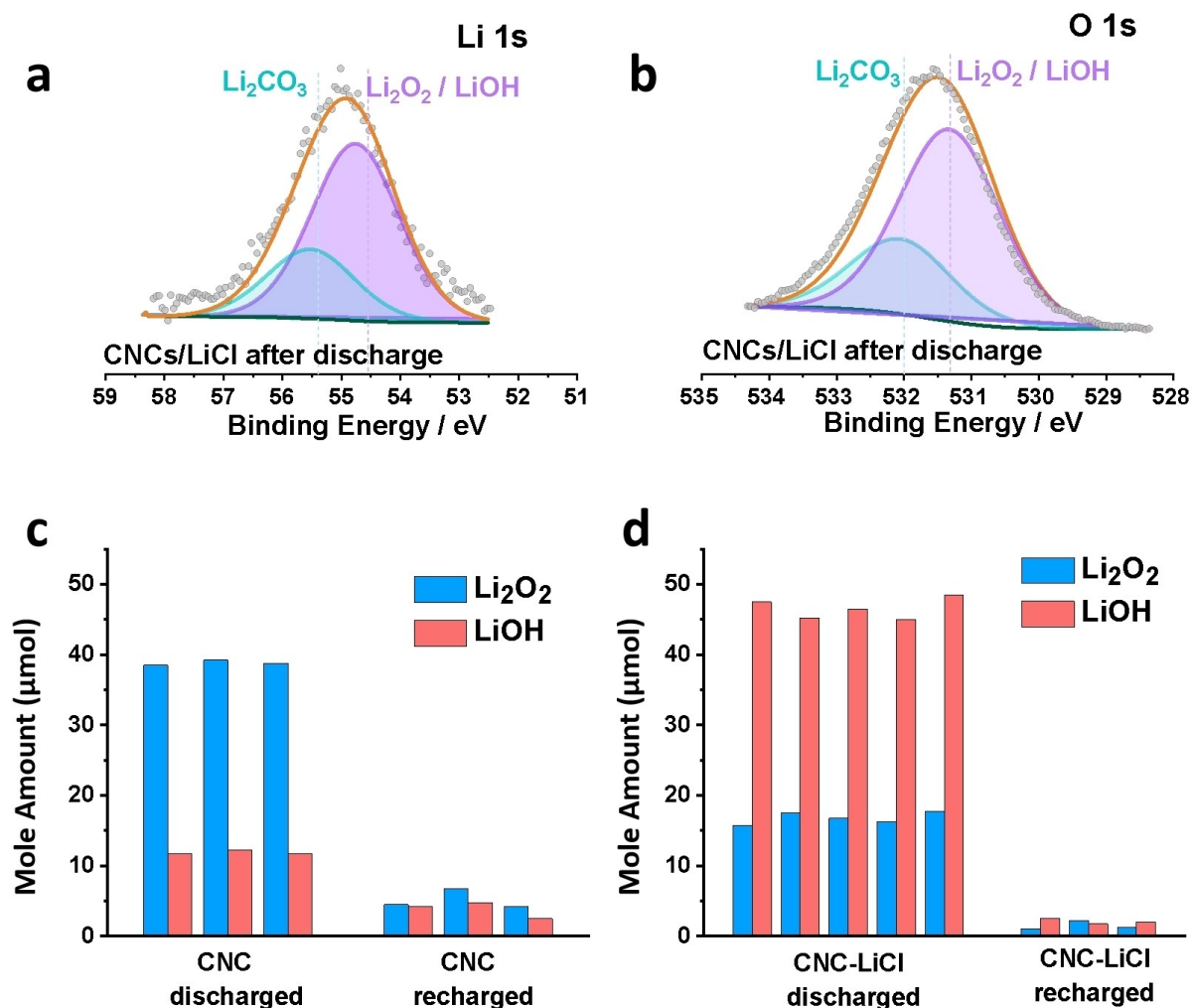
Figure 4. XPS spectra of a) Li 1s and b) O 1s of the discharged cathode with the LiCl as electrolyte additive. The iodometric titrations quantify the amount of deposited Li_2O_2 and LiOH on the c) CNC and d) CNC-LiCl cathode. Combined with the acid/base titrations, accurate amounts of LiOH are also shown for comparison.

iodine (the titrated target).[49–50] The detailed titration process was shown in the Supporting Information. In the absence of Cl^- (Figure 4c), the Li_2O_2 species were the main discharge products (average ~38.83 μmol), along with some LiOH (average ~11.92 μmol) could be detected, consistent with the products distribution in the DMSO based electrolyte reported previously.[51] On the contrary, when adding LiCl into the electrolyte, the LiOH product (average ~46.55 μmol) was increased obviously and the amount of Li_2O_2 species (average ~17.20 μmol) significantly reduced. This indicates that the addition of Cl^- can essentially change the typical aprotic oxygen reduction pathway by modulating the discharge products from Li_2O_2 to LiOH. It has been reported that the formation of LiOH products can enhance the kinetics of the charge process to achieve low charge overpotential. For example, Peng's group[9] measured the ionic (σ_{ion}) and electronic (σ_{eon}) conductivity of both Li_2O_2 and LiOH, revealing higher σ_{ion} and σ_{eon} of LiOH compared to that of Li_2O_2. To give further insight into the electrochemical reaction kinetics of the ORR process, the electrochemical impedance spectroscopy (EIS)

of Li–O_2 batteries before and after cycling with different electrolytes were also tested (Figure S7). It is found that the impedances of both Li–O_2 batteries with and without Cl^- additives are almost the same before discharge (Table S1, 55.6 vs. 59.7 $\Omega\,cm^{-2}$). However, after discharge, the impedance of the cell with Cl^- increased slightly to 179.8 $\Omega\,cm^{-2}$, while the impedance of the cell without Cl^- additives increased dramatically to 722.8 $\Omega\,cm^{-2}$ (Figure S7b). We propose that the Cl^- additive facilitates the solid-solid phase conversion from Li_2O_2 to LiOH, which possesses a better electrical conductivity than that of the bulk Li_2O_2.[9] Therefore, the reduction of impedance mainly originates from the formation of LiOH. Therefore, the cell with added Cl^- has significantly reduced charge overpotential and enhanced rate capability as shown in Figure 2. Meanwhile, after recharging the LiOH and Li_2O_2 discharge products almost decompose fully with Cl^-. In contrast, for the LiCl-free condition, the amount of LiOH is only reduced slightly, consistent with the Raman, XRD, and SEM results (Figure 3). As such, we propose that the discharge products can be effectively

decomposed, which were mediated by oxidized-chloride species during charge process.

It is crucial to confirm the reactivity of a related oxidized chloride species (Cl_3^- and Cl_2) toward the oxidization of corresponding discharge products ($LiOH/Li_2O_2$). The cyclic voltammetry (CV) curves of $Li-O_2$ cells with LiCl electrolyte under both oxygen (Figure 5a) and argon (Figure S8) atmospheres show two distinguishable oxidation peaks at about 3.3 V and 3.7 V, which correspond to the redox couples of Cl^-/Cl_3^- and Cl_3^-/Cl_2, respectively.[52] After assigning the corresponding chloride-related redox couples to the relevant charging plateaus at ~3.3 V (Figure 2a), we focus on the catalytic reactivity of the Cl^-/Cl_3^- OER redox couple. The equilibrium potential of LiOH depends on the composition of the electrolyte and additives. It was reported that the equilibrium potential of LiOH can be roughly estimated to be ~3.20 V in the DMSO solvent, considering a concentration of 100 p.p.m. of H_2O in the electrolyte.[53] It is lower than the oxidation peaks corresponding to the redox couples of Cl^-/Cl_3^- (3.3 V). Therefore, it is speculated that a chloride-mediated

LiOH decomposition reaction is caused by the chemical oxidation of LiOH via Cl_3^- to form Li^+, O_2, and H_2O (Figure 5c). Furthermore, the batteries with and without LiCl were charged directly as shown in Figure 5b, further demonstrating that such low charge overpotential is caused by the oxidation of discharge products rather than the oxidation of the additive Cl^- itself. Additionally, the charge capacity caused by the Cl^- is much lower than the capacity generated by the decomposition of discharge products (Figure 2b).

We propose a new mechanism to explain the OER and ORR process in aprotic $Li-O_2$ battery with LiCl as a redox mediator (Figure 5c and Supporting Information). During the discharge process, O_2 first accepts one electron to be reduced to superoxide (O_2^-),[54–55] which combines with Li^+ to form surface-adsorbed $LiO_{2(ads)}$ and/or soluble $LiO_{2(sol)}$ in the solution. Then, these discharge intermediates undergo a second electron transfer on the electrode surface or a disproportionation reaction in the solution to form a solid product, Li_2O_2, which has been intensively studied.[41,56] The generation of LiOH can be promoted via the help of Cl^- catalyst. The source of
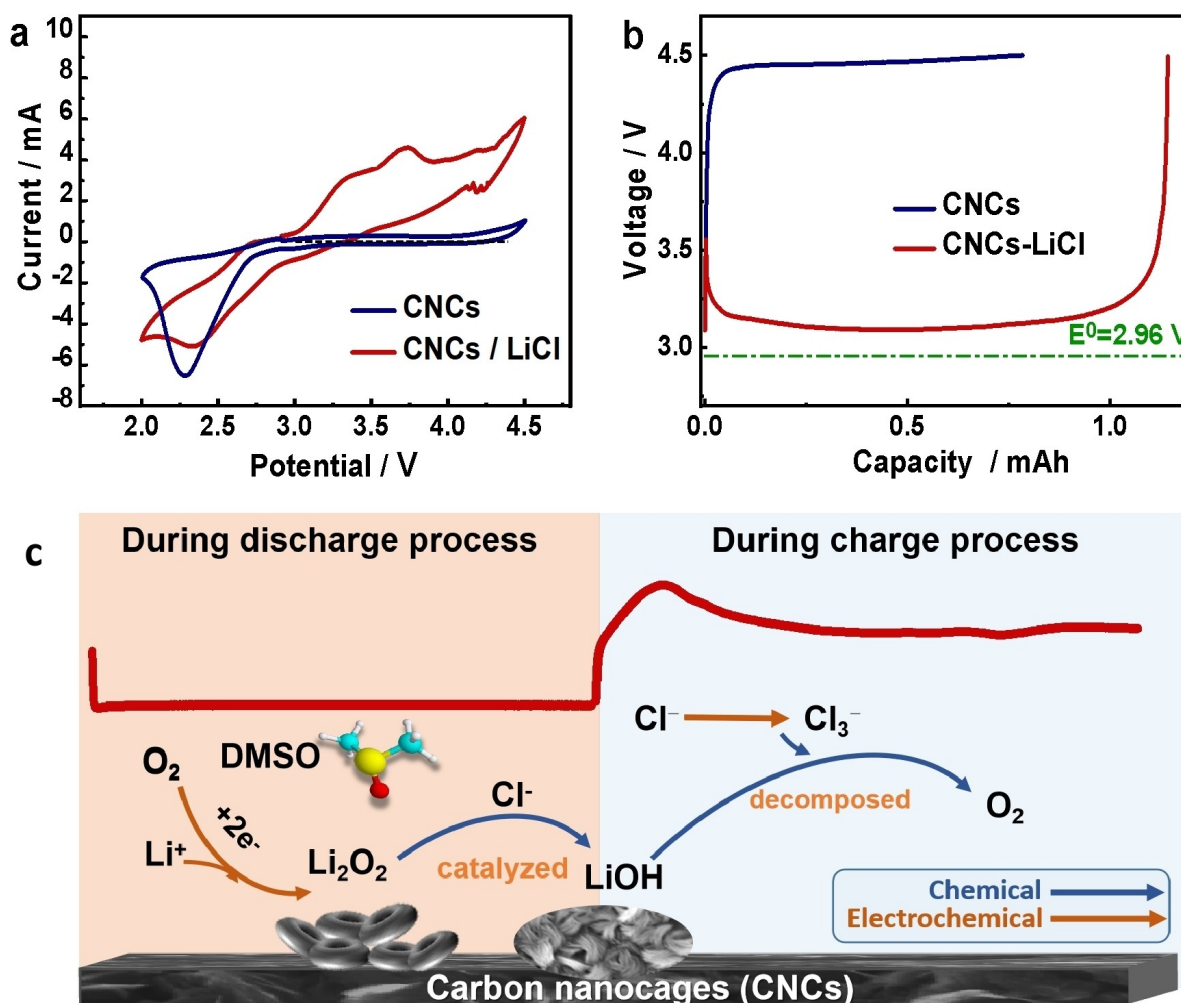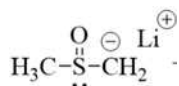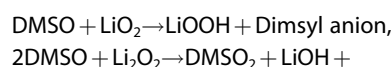

Figure 5. a) CV curves of CNCs and CNCs-LiCl cells at a scan rate of 2.2 mV s^{-1} within a voltage window of 2.0-4.5 V under oxygen atmosphere. b) Charge voltage curves of $Li-O_2$ batteries using CNCs as an electrode with $LiClO_4$ (blue) and LiCl:$LiClO_4$ = 1:9 (red) in the DMSO electrolyte at a current density of 100 mA g^{-1}. c) Schematic for the proposed discharge/charge processes of the CNCs-LiCl cell.

Batteries & Supercaps

Articles
doi.org/10.1002/batt.202000198

Chemistry
Europe
European Chemical
Societies Publishing

hydrogen atoms in the LiOH product comes from two possibilities, including the residual water from the electrolyte and the decomposition of DMSO electrolytes. It is well known that DMSO is able to react with superoxide-like species, through:[51,57]

$$DMSO + LiO_2 \rightarrow LiOOH + \text{Dimsyl anion,}$$
$$2DMSO + Li_2O_2 \rightarrow DMSO_2 + LiOH +$$

During the charge process, Li_2O_2 first undergoes a delithiation process to form O_2^-. Simultaneously, Cl^- is first oxidized to Cl_3^- at around 3.3 V. Then, the chloride-mediated LiOH and Li_2O_2 decomposition reactions are driven by Cl^-/Cl_3^- OER redox couple. H_2O will be generated after the decomposition of the LiOH, which will further react with LiO_2 to generate LiOH during the ORR process. These cyclic reactions occur continuously until the discharge products Li_2O_2 and LiOH decompose completely. Before a sufficient amount of Cl_3^- is formed, the decomposition of Li_2O_2 via a delithiation process is not energetically favorable. It requires the energy barrier for Li desorption along with the solvation of O_2^-, as shown in Figure 5c.[58–59] Further studies are needed to corroborate the proposed mechanism.

3. Conclusions

In summary, we have systemically investigated the influence of Cl^- additive on the discharging/charging behavior of $Li–O_2$ batteries. It is found that the formation of discharge product LiOH is promoted in the presence of Cl^- in the aprotic electrolyte and the Cl^- additive serves as the redox mediator during the charging process. The LiOH can be decomposed effectively through the Cl^-/Cl_3^- redox couple mediated oxidization with faster kinetics. The cell with Cl^- additive enables a considerably lower charge overpotential (~ 0.3 V), a long-cycle capability (up to 71 cycles) at 500 mA g^{-1} with a fixed capacity of 500 mAh g^{-1} and an impressive rechargeability. Our study provides a facile strategy toward the use of a redox mediator to achieve an ultra-low charge overpotential and high-rate and cycle performance of $Li–O_2$ batteries, thereby showing great potential to afford practical $Li–O_2$ batteries.

Conflict of Interest

The authors declare no conflict of interest.

[1] P. G. Bruce, S. A. Freunberger, L. J. Hardwick, J. M. Tarascon, *Nat. Mater.* **2011**, *11*, 19–29.

[2] Y. Xiao, X. Zhao, X. Wang, D. Su, S. Bai, W. Chen, S. Fang, L. Zhou, H. M. Cheng, F. Li, *Adv. Eng. Mater.* **2020**, *10*, 2000666.

[3] F. Li, J. Chen, *Adv. Eng. Mater.* **2017**, *7*, 1602934.

[4] Z. Zhang, J. Bao, C. He, Y. Chen, J. Wei, Z. Zhou, *Adv. Funct. Mater.* **2014**, *24*, 6826–6833.

[5] R. Black, B. Adams, L. F. Nazar, *Adv. Eng. Mater.* **2012**, *2*, 801–815.

[6] Y.-C. Lu, B. M. Gallant, D. G. Kwabi, J. R. Harding, R. R. Mitchell, M. S. Whittingham, Y. Shao-Horn, *Energy Environ. Sci.* **2013**, *6*, 750–768.

[7] O. Gerbig, R. Merkle, J. Maier, *Adv. Mater.* **2013**, *25*, 3129–3133.

[8] J. Wang, Y. Zhang, L. Guo, E. Wang, Z. Peng, *Angew. Chem. Int. Ed.* **2016**, *55*, 5201–5205; *Angew. Chem.* **2016**, *128*, 5287–5291.

[9] S. Ma, J. Wang, J. Huang, Z. Zhou, Z. Peng, *Angew. Chem. Int. Ed.* **2018**, *9*, 3333–3339.

[10] T. Liu, Z. Liu, G. Kim, J. T. Frith, N. Garcia-Araez, C. P. Grey, *Angew. Chem. Int. Ed.* **2017**, *56*, 16057–16062; *Angew. Chem.* **2017**, *129*, 16273–16278.

[11] T. Liu, M. Leskes, W. Yu, A. J. Moore, L. Zhou, P. M. Bayley, G. Kim, C. P. Grey, *Science* **2015**, *350*, 530–533.

[12] R. Gao, X. Liang, P. Yin, J. Wang, Y. L. Lee, Z. Hu, X. Liu, *Nano Energy* **2017**, *41*, 535–542.

[13] J. Lu, Y. J. Lee, X. Luo, K. C. Lau, M. Asadi, H. H. Wang, S. Brombosz, J. Wen, D. Zhai, Z. Chen, D. J. Miller, Y. S. Jeong, J. B. Park, Z. Z. Fang, B. Kumar, A. Salehi-Khojin, Y. K. Sun, L. A. Curtiss, K. Amine, *Nature* **2016**, *529*, 377–382.

[14] W. Dai, X. Cui, Y. Zhou, Y. Zhao, L. Wang, L. Peng, W. Chen, *Small Methods* **2019**, *3*, 1800358.

[15] W. Fan, B. Wang, X. Guo, X. Kong, J. Liu, *Nano Energy* **2016**, *27*, 577–586.

[16] Z. Lyu, T. Wang, R. Guo, Y. Zhou, J. Chen, X. Wang, M. Lin, X. Tian, M. Lai, L. Peng, L. Wang, Z. Peng, W. Chen, *J. Mater. Chem. A* **2019**, *7*, 10389–10396.

[17] Y. G. Zhu, Q. Liu, Y. Rong, H. Chen, J. Yang, C. Jia, L. J. Yu, A. Karton, Y. Ren, X. Xu, S. Adams, Q. Wang, *Nat. Commun.* **2017**, *8*, 14308.

[18] M. Tułodziecki, G. M. Leverick, C. V. Amanchukwu, Y. Katayama, D. G. Kwabi, F. Bardé, P. T. Hammond, Y. Shao-Horn, *Energy Environ. Sci.* **2017**, *10*, 1828–1842.

[19] Y. Zhou, Z. Lyu, Z. Liu, W. Dai, R. Guo, J. Yang, X. Cui, Y. Zhao, M. Lin, L. Peng, Z. Peng, W. Chen, *J. Mater. Chem. A* **2019**, *7*, 8777–8784.

[20] N. B. Aetukuri, B. D. McCloskey, J. M. Garcia, L. E. Krupp, V. Viswanathan, A. C. Luntz, *Nat. Chem.* **2015**, *7*, 50–56.

[21] Y. Qiao, S. Wu, J. Yi, Y. Sun, S. Guo, S. Yang, P. He, H. Zhou, *Angew. Chem. Int. Ed.* **2017**, *56*, 4960–4964; *Angew. Chem.* **2017**, *129*, 5042–5046.

[22] K. Liao, S. Wu, X. Mu, Q. Lu, M. Han, P. He, Z. Shao, H. Zhou, *Adv. Mater.* **2018**, 1705711.

[23] J. B. Park, S. H. Lee, H. G. Jung, D. Aurbach, Y. K. Sun, *Adv. Mater.* **2018**, *30*, 1704162.

[24] W. H. Ryu, F. S. Gittleson, J. M. Thomsen, J. Li, M. J. Schwab, G. W. Brudvig, A. D. Taylor, *Nat. Commun.* **2016**, *7*, 12925.

[25] Y. Ko, H. Park, B. Kim, J. S. Kim, K. Kang, *Trends Chem.* **2019**, *1*, 349–360.

[26] T. Zhang, K. Liao, P. He, H. Zhou, *Energy Environ. Sci.* **2016**, *9*, 1024–1030.

[27] H.-D. Lim, B. Lee, Y. Zheng, J. Hong, J. Kim, H. Gwon, Y. Ko, M. Lee, K. Cho, K. Kang, *Nat. Energy* **2016**, *1*, 16066.

[28] W.-J. Kwak, D. Hirshberg, D. Sharon, M. Afri, A. A. Frimer, H.-G. Jung, D. Aurbach, Y.-K. Sun, *Energy Environ. Sci.* **2016**, *9*, 2334–2345.

[29] Z. Liang, Y. C. Lu, *J. Am. Chem. Soc.* **2016**, *138*, 7574–7583.

[30] W. Zhang, Y. Shen, D. Sun, Z. Huang, J. Zhou, H. Yan, Y. Huang, *Nano Energy* **2016**, *30*, 43–51.

[31] M. Yu, X. Ren, L. Ma, Y. Wu, *Nat. Commun.* **2014**, *5*, 5111.

[32] X. P. Zhang, Y. N. Li, Y. Y. Sun, T. Zhang, *Angew. Chem. Int. Ed.* **2019**, *58*, 18394–18398.

[33] C. M. Burke, R. Black, I. R. Kochetkov, V. Giordani, D. Addison, L. F. Nazar, B. D. McCloskey, *ACS Energy Lett.* **2016**, *1*, 747–756.

[34] T. Liu, G. Kim, E. Jónsson, E. Castillo-Martinez, I. Temprano, Y. Shao, J. Carretero-González, R. N. Kerber, C. P. Grey, *ACS Catal.* **2018**, *9*, 66–77.

[35] S. Matsuda, Y. Kubo, K. Uosaki, K. Hashimoto, S. Nakanishi, *J. Phys. Chem. C* **2016**, *120*, 13360–13365.

[36] H. Deng, Y. Qiao, X. Zhang, F. Qiu, Z. Chang, P. He, H. Zhou, *J. Mater. Chem. A* **2019**, *7*, 17261–17265.

Batteries & Supercaps

Articles
doi.org/10.1002/batt.202000198

Chemistry Europe
European Chemical
Societies Publishing

[37] J. Zhang, B. Sun, Y. Zhao, K. Kretschmer, G. Wang, *Angew. Chem. Int. Ed.* **2017**, *56*, 8505–8509; *Angew. Chem.* **2017**, *129*, 8625–8629.

[38] K. Xie, X. Qin, X. Wang, Y. Wang, H. Tao, Q. Wu, L. Yang, Z. Hu, *Adv. Mater.* **2012**, *24*, 347–352.

[39] Q. Wu, L. Yang, X. Wang, Z. Hu, *Adv. Mater.* **2019**, 1904177.

[40] M. Liu, H. Fan, O. Zhuo, J. Chen, Q. Wu, L. Yang, L. Peng, X. Wang, R. Che, Z. Hu, *Nano Energy* **2020**, *68*, 104368.

[41] L. Johnson, C. Li, Z. Liu, Y. Chen, S. A. Freunberger, P. C. Ashok, B. B. Praveen, K. Dholakia, J. M. Tarascon, P. G. Bruce, *Nat. Chem.* **2014**, *6*, 1091–1099.

[42] B. J. Bergner, A. Schurmann, K. Peppler, A. Garsuch, J. Janek, *J. Am. Chem. Soc.* **2014**, *136*, 15054–15064.

[43] D. Wang, F. Zhang, P. He, H. Zhou, *Angew. Chem. Int. Ed.* **2019**, *58*, 2355–2359.

[44] F. S. Gittleson, K. P. C. Yao, D. G. Kwabi, S. Y. Sayed, W.-H. Ryu, Y. Shao-Horn, A. D. Taylor, *ChemElectroChem* **2015**, *2*, 1446–1457.

[45] F. S. Gittleson, W. H. Ryu, A. D. Taylor, *ACS Appl. Mater. Interfaces* **2014**, *6*, 19017–19025.

[46] D. Xiao, S. Dong, J. Guan, L. Gu, S. Li, N. Zhao, C. Shang, Z. Yang, H. Zheng, C. Chen, R. Xiao, Y.-S. Hu, H. Li, G. Cui, L. Chen, *Adv. Eng. Mater.* **2015**, *5*.

[47] L. Zhong, R. R. Mitchell, Y. Liu, B. M. Gallant, C. V. Thompson, J. Y. Huang, S. X. Mao, Y. Shao-Horn, *Nano Lett.* **2013**, *13*, 2209–2214.

[48] K. P. C. Yao, D. G. Kwabi, R. A. Quinlan, A. N. Mansour, A. Grimaud, Y.-L. Lee, Y.-C. Lu, Y. Shao-Horn, *J. Electrochem. Soc.* **2013**, *160*, A824-A831.

[49] R. Black, S. H. Oh, J. H. Lee, T. Yim, B. Adams, L. F. Nazar, *J. Am. Chem. Soc.* **2012**, *134*, 2902–2905.

[50] B. D. McCloskey, A. Valery, A. C. Luntz, S. R. Gowda, G. M. Wallraff, J. M. Garcia, T. Mori, L. E. Krupp, *J. Phys. Chem. Lett.* **2013**, *4*, 2989–2993.

[51] D. G. Kwabi, T. P. Batcho, C. V. Amanchukwu, N. Ortiz-Vitoriano, P. Hammond, C. V. Thompson, Y. Shao-Horn, *J. Phys. Chem. Lett.* **2014**, *5*, 2850–2856.

[52] A. Cerquetti, P. Longhi, T. Mussini, G. Natta, *J. Electroanal. Chem. Interfacial Electrochem.* **1969**, *20*, 411–418.

[53] F. Li, S. Wu, D. Li, T. Zhang, P. He, A. Yamada, H. Zhou, *Nat. Commun.* **2015**, *6*, 7843.

[54] Y. Wang, N.-C. Lai, Y.-R. Lu, Y. Zhou, C.-L. Dong, Y.-C. Lu, *Joule* **2018**, *2*, 2364–2380.

[55] Z. Peng, S. A. Freunberger, L. J. Hardwick, Y. Chen, V. Giordani, F. Barde, P. Novak, D. Graham, J. M. Tarascon, P. G. Bruce, *Angew. Chem. Int. Ed.* **2011**, *50*, 6351–6355; *Angew. Chem.* **2011**, *123*, 6475–6479.

[56] D. Aurbach, B. D. McCloskey, L. F. Nazar, P. G. Bruce, *Nat. Energy* **2016**, *1*, 16128.

[57] D. Sharon, M. Afri, M. Noked, A. Garsuch, A. A. Frimer, D. Aurbach, *J. Phys. Chem. Lett.* **2013**, *4*, 3115–3119.

[58] R. Liu, Y. Lei, W. Yu, H. Wang, L. Qin, D. Han, W. Yang, D. Zhou, Y. He, D. Zhai, B. Li, F. Kang, *ACS Energy Lett.* **2017**, *2*, 313–318.

[59] Y. Yang, G. Zheng, S. Misra, J. Nelson, M. F. Toney, Y. Cui, *J. Am. Chem. Soc.* **2012**, *134*, 15387–15394.